

# Increasing the imaging capabilities of multimode fibers by exploiting the properties of highly scattering media

Ioannis N. Papadopoulos,\* Salma Farahi, Christophe Moser, and Demetri Psaltis

School of Engineering, École Polytechnique Fédérale de Lausanne (EPFL), Station 17, 1015 Lausanne, Switzerland

\*Corresponding author: ioannis.papadopoulos@epfl.ch

Received March 11, 2013; revised June 27, 2013; accepted July 1, 2013;

posted July 3, 2013 (Doc. ID 186707); published July 26, 2013

We present a design that exploits the focusing properties of scattering media to increase the resolution and the working distance of multimode fiber (MMF)-based imaging devices. Placing a highly scattering medium in front of the distal tip of the MMF enables the formation of smaller sized foci at increased working distances away from the fiber tip. We perform a parametric study of the effect of the working distance and the separation between the fiber and the scattering medium on the focus size. We experimentally demonstrate submicrometer focused spots as far away as 800  $\mu\text{m}$  with 532 nm light. © 2013 Optical Society of America

OCIS codes: (060.2350) Fiber optics imaging; (070.5040) Phase conjugation; (090.1995) Digital holography; (110.7050) Turbid media.

<http://dx.doi.org/10.1364/OL.38.002776>

Endomicroscopy is a powerful technique that can help clinicians in diagnosis and surgery [1]. Among the different designs suggested for endoscopes, clinically available ones are generally based on fiber bundles in which each single-mode fiber core acts as a single pixel of the final image [2]. Another category of endoscopes is built by combining a single-mode fiber for delivery of excitation light, conventional optics and mechanical actuators for focusing and scanning, and finally a multimode fiber (MMF) for collection of the fluorescent signal [3]. Recently, considerable attention has been drawn toward MMFs that appear as promising candidates for high-resolution minimally invasive endoscopic imaging [4–7]. The large number of degrees of freedom present in a MMF allows for the transmission of large amounts of information, while at the same time its size remains relatively small. The overall diameter of the MMF device can be limited to less than 500  $\mu\text{m}$ .

The new family of MMF-based endoscopes proposed recently can be used with different working distances. However, as was demonstrated in [5,7], there is a clear trade-off between working distance and achievable resolution. This is because the resolution is directly linked to the numerical aperture (NA); therefore as the physical aperture of the MMF remains constant, the image quality achieved by such a system deteriorates as the working distance increases.

It has been demonstrated that scattering media under the appropriate control of the incident wavefront can be used to focus light [8,9], transmit an image [10], rotate the polarization [11], or act as mirrors [12]. Based on wavefront shaping techniques, even opaque layers of scattering media can be rendered transparent as far as the information transmission is concerned. The optical field propagating through a scattering medium on its way to a focus spot on the other side of the scatterer gets coupled to a broader spectrum of spatial frequencies compared to the incident beam. Different groups have exploited this effect to demonstrate an enhancement of the NA of optical systems [8,13,14].

In this Letter, we demonstrate that a scattering medium used in conjunction with an MMF imaging system can increase the working distance and the associated field of view while maintaining a high lateral resolution. Our approach is based on the synergetic exploitation of an MMF and a highly scattering medium placed in front of the fiber, so that the effective number of degrees of freedom of the system is increased. We use digital phase conjugation (DPC) [9,15–17] to calculate the appropriate wavefront that will bring light into focus after it propagates through the fiber and the scattering medium.

The experimental implementation of the suggested scheme is depicted in Fig. 1. A highly scattering medium is placed in front of the distal tip of the multimode optical fiber (200  $\mu\text{m}$  core diameter MMF) at a specific distance

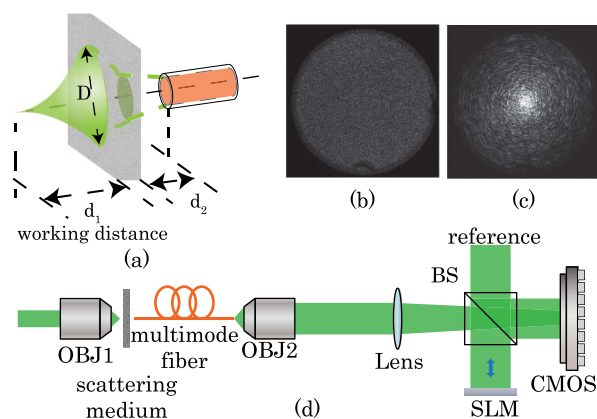


Fig. 1. (a) Highly scattering medium placed in front of an MMF will lead to a system with an increased number of degrees of freedom. The fiber diffracts with an angle associated with the fiber NA and enters the scattering medium, where it gets diffused. The large aperture from which the focusing originates is a result of these two processes. (b),(c) Comparison of the speckled output of the fiber with and without the scattering medium. The presence of the scattering medium causes the maximum number of modes to be excited in the fiber in a uniform manner [shown in (b)]. (d) Experimental setup.

$d_2$ . The scattering medium used is a single layer of white paint of 20  $\mu\text{m}$  thickness deposited on a glass slide (150  $\mu\text{m}$  thick). The working distance,  $d_1$ , of the composite system is defined as the focusing distance away from the end surface of the glass slide. The experimental implementation of DPC is the same as the one described in [17]. A 532 nm continuous-wave diode pumped solid state (DPSS) laser source was used to generate a diffraction-limited spot at the desired distance away from the scattering medium. The optical field propagates through the ensemble of the scattering medium and the MMF and reaches the proximal tip of the fiber. The output of the fiber is imaged and holographically recorded on a CMOS digital sensor; the phase is extracted through the digital reconstruction in the computer and then assigned onto the phase-only spatial light modulator (SLM) device. The reference beam is reflected off the SLM, picking up the calculated phase information and thus forming the optical phase conjugate beam. The phase conjugate beam backpropagates first through the MMF and then through the scattering medium, forming a sharp focused spot at the original position.

As can be seen in Fig. 1(a), the presence of the scattering medium has a double effect on the final aperture of the system,  $D$ . Initially the optical field exits the fiber and is diffracted with an angle equal to the NA of the fiber, and as it propagates inside the turbid medium it experiences multiple scattering and exits with an increased aperture compared to the entering one. The width of the output aperture depends on the diffraction angle of the fiber and the thickness of the scattering medium. Moreover, the size of the focused spot will be defined by the size of the final output aperture of the system and the working distance.

In Figs. 1(b) and 1(c) we compare the speckle output of the fiber at the proximal tip with and without the scattering medium. We can observe that the presence of the scattering medium causes a greater number of modes to be excited in the fiber in a uniform manner manifested by the uniform smaller speckles that are shown in Fig. 1(b).

Based on the above physical description, we can predict that for a fixed focal distance, the size of the spot will become smaller as the distance between the fiber end and the scatterer is increased. On the other hand, for a fixed distance between the fiber and the scattering medium, the aperture of the system remains constant and therefore the beam waist of the focused spot will increase with increasing working distance.

In order to better quantify this behavior, we perform a parametric study of the focus size versus the distances  $d_1$  and  $d_2$ . The resulting focused spot after DPC is imaged onto a CCD sensor, and the measured data are used as an input to a Gaussian curve-fitting algorithm. The calculated beam waist is defined as the  $2 * w_0$  parameter of the fitted Gaussian profile.

The results demonstrated in Fig. 2 verify the expected behavior. Figures 2(a)–2(e) show the evolution of the generated focus at a working distance of 600  $\mu\text{m}$  as the distance between the scattering medium and the fiber is changed from 200 to 1000  $\mu\text{m}$ . The focused spots have a shape very close to the ideally expected Gaussian. On the right-hand side of Fig. 2, a summarized plot of all the measured results is presented. As can be observed, for any

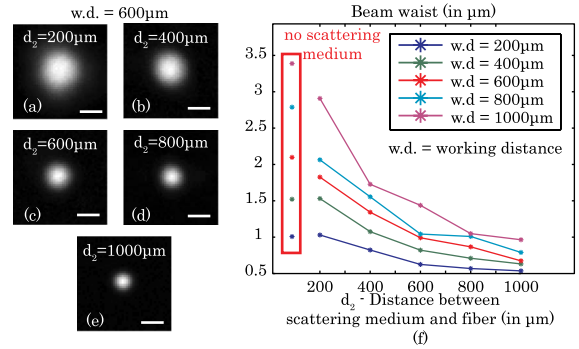


Fig. 2. (a)–(e) Evolution of the beam size for a fixed working distance of 600  $\mu\text{m}$  as the distance between the scattering medium and the fiber increases from 200 to 1000  $\mu\text{m}$ . The spot has the expected Gaussian profile, and a beam waist smaller than 1  $\mu\text{m}$  is demonstrated. Scale bar is 1  $\mu\text{m}$ . (f) Quantitative results of the Gaussian fitted beam waist as a function of the distance between the fiber and the scattering medium for different working distances. As expected, the beam waist decreases when the fiber is moved away from the scattering medium.

certain working distance of the final device, an increase in the distance between the fiber and the scatterer signifies a decrease in the beam waist of the generated spot. The effect is very prominent, especially when the focus is generated at 800 and 1000  $\mu\text{m}$ , where we can see that spot sizes even smaller than 1  $\mu\text{m}$  are achieved.

The effect of placing a scattering medium in front of the fiber output is to increase the effective NA of the system by directly increasing the physical output aperture from which the focus is generated and also to enable coupling between high- to low-order modes that can propagate through the fiber. However, unlike a conventional lens, a free-space scattering medium behaves in a spatially invariant stochastic way, meaning that the number of modes that will be excited in the scattering medium when any given optical field propagates through does not depend on the relative lateral position of the optical field to the scattering medium.

In Fig. 3 a superimposed image of digitally scanned focused spots across a field of view of 256  $\mu\text{m}$  by 192  $\mu\text{m}$  is presented. We can observe that the quality and size of the generated foci do not degrade as the spot is moved away

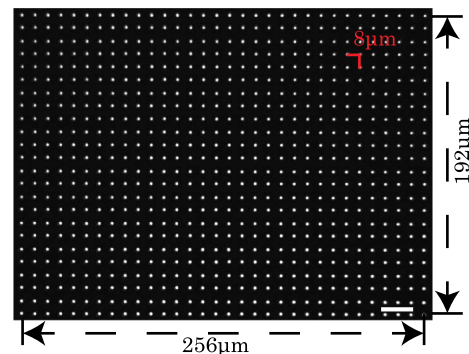


Fig. 3. Superimposed images of focused spots generated across a 256  $\mu\text{m}$   $\times$  192  $\mu\text{m}$  field of view, at a working distance of 600  $\mu\text{m}$  (distance between fiber and diffuser,  $d_2 = 600 \mu\text{m}$ ; distance between adjacent spots = 8  $\mu\text{m}$ ). The size and quality of the spots remain constant across the whole field of view. Scale bar, 20  $\mu\text{m}$ .

from the center and toward the edges of the field of view. As a result of this, the application of DPC on the combination of a scattering medium and a MMF transforms it into a device capable of rendering high-quality, aberration-free, focused spots across a large field of view.

In order to perform imaging with the suggested technique, the major prerequisite is that the generated focused spots must have a sufficient signal-to-noise ratio (SNR) compared to the background. As can be verified by the images shown and measurements performed, the estimated SNR (defined as the maximum of the focus over the mean of the background) is in average higher than 2000:1. A potential difficulty arising from the suggested geometry is the fact that the scattering phenomena both during focusing and during light collection for imaging decrease the expected photon budget. For the scattering medium used, the transmission attenuation was measured to be around 25 dB. This can be overcome by increasing the power of the excitation laser source or by using a scatterer with a smaller scattering coefficient. A different approach could be to use a notch filter with a surrounding annular scattering ring in a dark-field configuration where we can exploit the annular ring for the generation of the focused spot, while on the collection part, most of the fluorescent light will be captured by the fiber.

As has been demonstrated previously, MMF imaging devices are capable of delivering high-resolution images in an ultrathin endoscopic device. However, the NA of the fiber used limits the resolution and working distance of these devices. The scheme suggested and implemented in this Letter has been shown to help mitigate those problems through the increase of the effective NA of the final device, by augmenting the physical aperture of the system and by enabling the transfer of information from high- to low-order modes that can propagate in the fiber. The decreased size of the achieved focused spots at increasing working distances across a large field of view highly enhances the imaging capabilities of MMF-based endoscopes.

MMF-based imaging devices can be useful in endoscopy in a rigid configuration. The transmission matrix of the optical system is highly distorted when the fiber is bent. In order to overcome this problem, these devices can be used in a rigid needle-type configuration where the MMF is housed inside a stainless steel needle tip. This needle tip prevents the fiber from moving when the endoscope is inserted inside a body cavity or inside tissue through direct penetration. At the same time, the needle

tip can be used for the integration of the scattering medium lens in front of the fiber, therefore enabling the fabrication of a passive, self-consistent endoscopic head. Also, a layer of tissue inside the area to be imaged can be used as the scatterer needed. In this case, however, the presence of a beacon that will probe the scattering medium is necessary.

In conclusion, we suggest a configuration in which a free-space scattering medium and an MMF work together to increase the resolution and working distance of fiber-based imaging systems. We have demonstrated that this configuration can lead to the generation of aberration-free submicrometer focused spots, 800  $\mu\text{m}$  away from the endoscopic head over an extended field of view of 256  $\mu\text{m}$  by 192  $\mu\text{m}$ .

This work was partially supported by the Bertarelli Foundation.

## References

1. B. A. Flusberg, E. D. Cocker, W. Piyawattanametha, J. C. Jung, E. L. Cheung, and M. J. Schnitzer, *Nat. Methods* **2**, 941 (2005).
2. A. F. Gmitro and D. Aziz, *Opt. Lett.* **18**, 565 (1993).
3. W. Göbel, J. N. D. Kerr, A. Nimmerjahn, and F. Helmchen, *Opt. Lett.* **29**, 2521 (2004).
4. S. Bianchi and R. Di Leonardo, *Lab Chip* **12**, 635 (2012).
5. T. Čížmár and K. Dholakia, *Nat. Commun.* **3**, 1027 (2012).
6. Y. Choi, C. Yoon, M. Kim, T. Yang, C. Fang-Yen, R. Dasari, K. Lee, and W. Choi, *Phys. Rev. Lett.* **109**, 12285 (2012).
7. I. N. Papadopoulos, S. Farahi, C. Moser, and D. Psaltis, *Biomed. Opt. Express* **4**, 260 (2013).
8. I. Vellekoop, A. Lagendijk, and A. P. Mosk, *Nat. Photonics* **4**, 320 (2010).
9. C.-L. Hsieh, Y. Pu, R. Grange, and D. Psaltis, *Opt. Express* **18**, 12283 (2010).
10. S. Popoff, G. Leroosey, M. Fink, A. C. Boccara, and S. Gigan, *Nat. Commun.* **1**, 1 (2010).
11. Y. Guan, O. Katz, E. Small, J. Zhou, and Y. Silberberg, *Opt. Lett.* **37**, 4663 (2012).
12. O. Katz, E. Small, and Y. Silberberg, *Nat. Photonics* **6**, 549 (2012).
13. Y. Choi, T. Yang, C. Fang-Yen, P. Kang, K. Lee, R. Dasari, M. Feld, and W. Choi, *Phys. Rev. Lett.* **107**, 023902 (2011).
14. E. G. van Putten, D. Akbulut, B. J. W. Vos, A. Lagendijk, and A. P. Mosk, *Phys. Rev. Lett.* **106**, 193905 (2011).
15. C. Bellanger, A. Brignon, J. Colineau, and J. P. Huignard, *Opt. Lett.* **33**, 2937 (2008).
16. M. Cui and C. Yang, *Opt. Express* **18**, 3444 (2010).
17. I. N. Papadopoulos, S. Farahi, C. Moser, and D. Psaltis, *Opt. Express* **20**, 10583 (2012).